

Stripe Instabilities of Geometries with Hyperscaling Violation

Norihiro IIZUKA^{1,*} and Kengo MAEDA^{2,†}

¹*Yukawa Institute for Theoretical Physics, Kyoto University, Kyoto 606-8502, JAPAN*

²*Faculty of Engineering, Shibaura Institute of Technology, Saitama 330-8570, JAPAN*

(Dated: June 15, 2021)

We study the dynamical stripe instabilities on the geometries with hyperscaling violation in the IR, which asymptotically approach AdS₄ in the UV. The instabilities break the translational invariance spontaneously and are induced by the axion term $\sim aF \wedge F$ in the bulk action. We first study the perturbation equations in the probe limit, and find that there is a strong correlation between the stripe instabilities caused by the axion term and parameters of the theories which determine the IR hyperscaling violation. Contrary to the IR AdS₂ case, the effect of the axion term for the stripe instabilities can be enhanced/suppressed at low temperature depending on the parameters. For a certain one-parameter family of the hyperscaling violation, we find the onset of the stripe instability analytically in the axion coupling tuned model. For more generic parameter range of hyperscaling violation, we study the instability onset by searching for the zero mode numerically on the full geometries. We also argue that quite analogous results hold, after taking into account the graviton fluctuation, *i.e.*, beyond the probe limit.

Contents

I. Introduction	1
II. Einstein-Maxwell-dilaton-axion system	2
A. The set-up	2
B. Background solutions	2
1. IR Hyperscaling violating geometries	2
2. Full solutions interpolating IR hyperscaling violating geometries to UV AdS ₄	3
III. Perturbation analysis in the probe limit	4
A. Perturbation equations in the probe limit	4
B. Negative momentum square mode on the hyperscaling violating geometry: finite temperature analysis	5
C. Zero temperature analysis and instability criteria	7
1. Zero temperature perturbation	7
2. Analytical criteria for instability onset for special type of hyperscaling violation	7
3. $\xi = 0$ case	8
D. Numerical analysis for the bulk zero mode on the full geometries	9
IV. Perturbation analysis beyond the probe limit	12
V. Summary and Discussion	13
Acknowledgments	14
References	15

I. INTRODUCTION

Holography is an extremely useful tool to understand the quantum field theory in the strongly coupled limit [1–3]. This motivates us to apply the holographic technique to interesting subjects such as QCD and condensed matter physics, and see what we can learn about real world physics from holography.

In studying the quantum field theories for QCD or condensed matter physics, one of the most important things is understanding the infrared (or vacuum) structure. For example, in many of the recent studies of the non-Fermi liquid in holographic setting, the most interesting nature is originated from its IR behavior, *i.e.*, the bulk black brane near horizon geometries [4–6]. This is natural from the trivial fact that Fermi surface is the low energy nature of the systems. In the holographic superconductor case [7–12], with or without various lattice effects [13–15], the most interesting features are their symmetry breaking pattern in the IR, *i.e.*, in the near horizons of hairy black branes. Another interesting aspects of black brane geometries for the condensed matter application is the existence of flux at the horizon, since this gives the violation of the Luttinger theorem for the field theory duals [16–21] and this resembles the fractionalized Fermi-liquids [19, 22, 23]. Therefore it gives the possibly interesting dual of them. Quantum criticality is another fine example where IR dominates the physics. In these ways, we are especially interested in the IR behavior of the black brane near horizon geometries in holographic condensed matter, and it is quite interesting to understand their various dynamics from the geometry side. See also [24, 25] for recent development of the classification of the black brane geometries which admits homogeneous but anisotropic geometries.

One of the most interesting geometries in this view point which people actively studied recently is Lifshitz geometry [26–28] and so-called geometry with hyperscaling violation [29–38]. These geometries are interesting

*iizuka@yukawa.kyoto-u.ac.jp

†maeda302@sic.shibaura-it.ac.jp

since they are, if realized in the IR, dual to the field theories which break the Lorentz-invariance but respect spatial rotation and translational invariance in the IR. IR Lifshitz and hyperscaling violating geometries can be realized as the near horizon geometries of some black brane solutions, and they can be obtained, for example, in theories where dilaton has run-away behavior governed by the exponential potentials [28–30].

Another interesting nature of these geometries is that these geometries do not admit large entropy unlike Reissner-Nordstrom black branes [55]. On the boundary field theory side, this means that it has vanishing entropy density at the zero temperature limit, which is more natural from thermodynamical view point. In addition, rich behavior of the hyperscaling violating geometries allows more exotic behavior for the fermion correlators. For examples, it gives various ω -dependence for the non-Fermi liquid decay-rates, as shown in [30].

In the meantime, recently a lot of recent progress was made in understanding the translational symmetry breaking in the holographic setting [40–47]. The symmetry breaking can be induced by the axion term $aF \wedge F$ in 4d gravity (where a is neutral pseudo-scalar field, and we call it axion in this paper), and can occur both spontaneously and by the source term. In many of the situations, the analysis is mainly done for the Reissner-Nordstrom black brane which admits AdS_2 geometries in the IR. Given this, it is very natural to study if above IR Lifshitz or geometries with hyperscaling violation can survive after we take into account such axion effect and see if it induces the translational symmetry breaking. Furthermore, since this instability changes the IR nature of the geometries, studying this instability on the hyperscaling violating geometries is by itself interesting questions as general relativity problem. In this paper, we study the instability on the IR hyperscaling violating geometries, focusing on the onset of the stripe instability.

The organization of this paper is as follows; We first review the geometries with hyperscaling violation in the 4d Einstein-Maxwell-dilaton-axion system in §II. The geometries with hyperscaling violation emerge in the IR, *i.e.*, in the near horizon limit of the full solutions which approach AdS_4 in the UV asymptotically. In §III, we study the perturbation on these geometries in the probe limit. We first analyze the perturbation focusing on the IR geometries at small nonzero temperature in §III B, and at zero temperature limit §III C 1. These studies allow us to find the dependence of the stripe instabilities on the parameters of the theories which determine the IR hyperscaling violation. Given this, we identify the instability onset on a certain one-parameter family of the hyperscaling violating geometries, in §III C 2. In §III D, we search for the zero mode on the full geometries for more generic parameters numerically. In §IV, we study the perturbation equations without taking the probe limit, and see that essentially the same results hold compared to the probe limit case. We end with a summary and discussion in §V.

II. EINSTEIN-MAXWELL-DILATON-AXION SYSTEM

A. The set-up

The action we consider is Einstein-Maxwell theory coupled to a dilaton-axion, given by

$$S = \int d^4x \sqrt{-g} (R - 2(\nabla\phi)^2 - 2e^{2\xi\phi}(\nabla a)^2 - V(\phi) - f(\phi)F_{\mu\nu}F^{\mu\nu} - \theta(a)F_{\mu\nu}\tilde{F}^{\mu\nu}). \quad (1)$$

Here, $\tilde{F}^{\mu\nu} \equiv \frac{1}{2}\epsilon^{\mu\nu\rho\kappa}F_{\rho\kappa}$, and $\epsilon^{\mu\nu\rho\kappa}$ has a factor of $1/\sqrt{-g}$ in its definition such that axion term $\theta(a)F_{\mu\nu}\tilde{F}^{\mu\nu}$ is independent of the metric. We take the convention that $\epsilon_{trxy} > 0$.

As an explicit example, in this paper we consider

$$f(\phi) = e^{2\alpha\phi}, \quad V(\phi) = 2V_0 \cosh 2\delta\phi, \quad \theta(a) = c_1 a, \quad (2)$$

for the explicit stability/symmetry breaking by taking various real parameters α , δ , c_1 , and V_0 , but we take $V_0 < 0$. Note that $V(\phi) \rightarrow V_0 e^{2\delta\phi}$ in the $\delta\phi \rightarrow \infty$ limit.

The Einstein equation in trace reversed form becomes

$$R_{\mu\nu} - 2\partial_\mu\phi\partial_\nu\phi - 2e^{2\xi\phi}\partial_\mu a\partial_\nu a = f(\phi) \left(2F_{\mu\lambda}F_\nu^\lambda - \frac{1}{2}g_{\mu\nu}F^2 \right) + \frac{1}{2}g_{\mu\nu}V(\phi, a), \quad (3)$$

which is irrelevant to the axionic $\theta(a)F \wedge F$ term. The equations of motion for dilaton and axion are

$$\frac{4}{\sqrt{-g}}\partial_\mu(\sqrt{-g}g^{\mu\nu}\partial_\nu\phi) = \partial_\phi V(\phi, a) + (\partial_\phi f(\phi))F^2 + 4\xi e^{2\xi\phi}(\nabla a)^2, \quad (4)$$

$$\frac{4}{\sqrt{-g}}\partial_\mu(\sqrt{-g}g^{\mu\nu}\partial_\nu a) = (\partial_a\theta(a))F\tilde{F}, \quad (5)$$

and for the gauge field, we have

$$\partial_\mu \left(\sqrt{-g} \left(f(\phi)F^{\mu\nu} + \theta(a)\tilde{F}^{\mu\nu} \right) \right) = 0, \quad (6)$$

with the Bianchi identity

$$\partial_\mu F_{\nu\lambda} + \partial_\nu F_{\lambda\mu} + \partial_\lambda F_{\mu\nu} = 0. \quad (7)$$

B. Background solutions

1. IR Hyperscaling violating geometries

First we review the background hyperscaling violating geometries [29, 30], on which we later add the small fluctuation to study its stability. We consider the background geometries where all quantities are functions of

only the radial direction r . By using the r coordinate re-definition, we make the metric in the form

$$ds^2 = -\tilde{a}(r)^2 dt^2 + \frac{dr^2}{\tilde{a}(r)^2} + b(r)^2(dx^2 + dy^2) \quad (8)$$

and equations of motion and the Bianchi identity are solved by

$$F = F_{tr}(r)dt \wedge dr, \quad F_{tr}(r) = \frac{Q_e}{b^2 f(\phi)}. \quad (9)$$

In the IR limit, we choose $\delta\phi \rightarrow \infty$, such that $V(\phi) \rightarrow V_0 e^{2\delta\phi}$. Then with the approximate potential $V(\phi) = V_0 e^{2\delta\phi}$ in IR, we can obtain the solutions as given by [30],

$$\tilde{a}(r)^2 = C_a^2 r^{2\gamma} \left(1 - \left(\frac{r_h}{r}\right)^{2\beta+2\gamma-1}\right), \quad (10)$$

$$b(r)^2 = r^{2\beta}, \quad \phi(r) = k \log r, \quad (11)$$

where

$$\beta = \frac{(\alpha + \delta)^2}{4 + (\alpha + \delta)^2}, \quad \gamma = 1 - \frac{2\delta(\alpha + \delta)}{4 + (\alpha + \delta)^2}, \quad (12)$$

$$k = -\frac{2(\alpha + \delta)}{4 + (\alpha + \delta)^2}, \quad Q_e^2 = -V_0 \frac{2 - \delta(\alpha + \delta)}{2(2 + \alpha(\alpha + \delta))}, \quad (13)$$

$$C_a^2 = -V_0 \frac{(4 + (\alpha + \delta)^2)^2}{2(2 + \alpha(\alpha + \delta))(4 + (3\alpha - \delta)(\alpha + \delta))}, \quad (14)$$

and axion field a is set to be zero, $a = 0$ [56]. There are parameter space which satisfies $Q_e^2 > 0$, $C_a^2 > 0$, $\gamma > 0$, $\gamma - \beta > 0$, $\beta > 0$ and $\delta k < 0$. The condition $\gamma > 0$ arises from the requirement that g_{tt} vanishes at the horizon in zero temperature limit, and $\gamma - \beta > 0$ arises from the null energy condition at the $r_h = 0$ case. $\beta > 0$ is automatically satisfied and $\delta k < 0$ is for $\delta\phi \rightarrow \infty$ at $r \rightarrow 0$, which gives $\delta(\alpha + \delta) > 0$.

The temperature T of the system is given in terms of r_h as

$$T = \frac{(2\gamma + 2\beta - 1)C_a^2}{4\pi} r_h^{2\gamma-1}. \quad (15)$$

So we require $\gamma > 1/2$ so that $r_h \rightarrow 0$ at $T \rightarrow 0$. Then, with $\beta > 0$, this geometry is thermodynamically stable since the horizon area vanishes at the zero temperature limit and dual theories satisfy the 3rd law of the thermodynamics.

In zero temperature limit, the metric reduces to

$$\tilde{a}(r) = C_a r^\gamma, \quad b(r) = r^\beta, \quad (16)$$

therefore the horizon locates at $r = 0$. This zero temperature metric is sometimes written as

$$ds_d^2 = \tilde{r}^{-\frac{2}{d}(d-\theta)} \left(-\tilde{r}^{-2(z-1)} dt^2 + l^2 d\tilde{r}^2 + dx^2 + dy^2 \right),$$

$$z = 1 - \frac{\gamma - \beta}{1 - \gamma - \beta}, \quad \theta = 4 \left(\frac{1 - \gamma}{1 - \gamma - \beta} \right), \quad (17)$$

$$l^2 = \frac{1}{(1 - \gamma - \beta)^2 C_a^2}, \quad (18)$$

by the coordinate transformation $\tilde{r} \equiv r^{1-\gamma-\beta}$, where $d = 4$.

These are the so-called ‘‘geometries with hyperscaling violation’’. The parameter z is called dynamical critical exponent and θ is called hyperscaling violation parameter. For generic values of α and δ , we have $\gamma \neq 1$ and $\theta \neq 0$. If $\gamma = 1$, and equivalently, $\theta = 0$, this IR metric has additional scale invariance symmetry, therefore θ characterizes the ‘‘deviation’’ from the scale invariant limit. Similarly, if $z = 1$, then time and spatial coordinate transform equivalently, therefore z characterizes the ‘‘deviation’’ from the relativistic limit.

Before we continue, let us pose to check the number of the parameters of our system. Our model, given by eq. (1) and (2), has 5 real parameters, α , δ , V_0 , ξ , c_1 . However V_0 is a parameter to set the scale (of asymptotic AdS₄), so we can set $V_0 = -1$, without loss of generality. Furthermore, since our background has zero VEV for the axion field, $a = 0$, parameters ξ and c_1 are irrelevant for the background. In this way, the background is characterized by two real parameters α and δ only. Especially in the IR, these two parameters determine the hyperscaling violation θ and z , or equivalently β and γ .

We will now review the full solutions which interpolate these IR β, γ geometries with hyperscaling violation to UV AdS₄ asymptotically.

2. Full solutions interpolating IR hyperscaling violating geometries to UV AdS₄

The solution we reviewed is the IR limit of the full solution which asymptotically approaches AdS₄ in UV. In order to obtain the full solution which connects the IR to UV, we perturb the IR solution by $O(\epsilon)$ and numerically follow the evolution of it. To obtain asymptotic AdS₄ with appropriate boundary conditions, we tune ϵ , where ϵ is a small parameter. In the zero temperature case, we set [30]

$$\tilde{a}(r) = C_a r^\gamma (1 + \epsilon d_1 r^\nu), \quad (19)$$

$$b(r) = r^\beta (1 + \epsilon d_2 r^\nu), \quad (20)$$

$$\phi(r) = k \log r + \epsilon d_3 r^\nu, \quad (21)$$

and the perturbation equations of motion are all satisfied up to the $O(\epsilon)$ by setting

$$\nu_1 = \nu_2 = \nu, \quad d_2 = \frac{B_1}{B_2} d_1, \quad (22)$$

$$d_3 = \frac{4(-1 + \nu) + (\alpha + \delta)^2(1 + \nu)}{4(\alpha + \delta)} d_2, \quad (23)$$

$$\nu = \frac{2(\delta(\alpha + \delta) + 2)}{(\alpha + \delta)^2 + 4} - \frac{3}{2} + \frac{A}{2((\alpha + \delta)^2 + 4)^2}, \quad (24)$$

$$A = \left([4 + (3\alpha - \delta)(\alpha + \delta)] [(\alpha + \delta)^2 + 4]^2 \right. \\ \left. \times (36 - (\alpha + \delta)(\alpha(8\delta(\alpha + \delta) - 19) + 17\delta)) \right)^{1/2}, \quad (25)$$

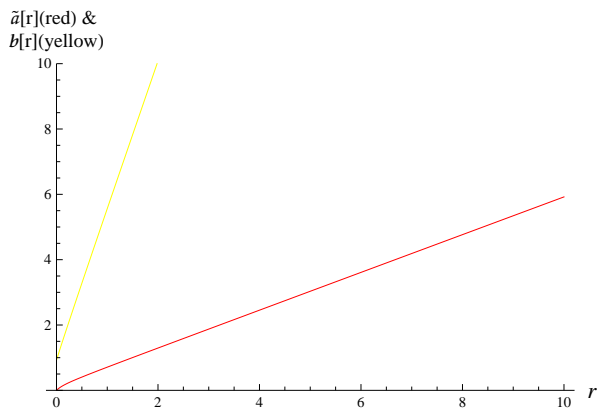


FIG. 1: The interpolating solution $\sqrt{-g_{tt}(r)} = \sqrt{g^{rr}(r)} = \tilde{a}(r)$ (red) and $\sqrt{g_{xx}(r)} = \sqrt{g_{yy}(r)} = b(r)$ (yellow) for the parameter choice $\alpha = -1/3$, $\delta = 0.55$, $d_1 = 0.01$, $V_0 = -1$. It shows $\lim_{r \rightarrow \infty} \tilde{a}(r) \rightarrow \frac{1}{\sqrt{3}}r$, and $\lim_{r \rightarrow \infty} b(r) \propto r$ as is expected from asymptotic AdS₄ in the UV. (color online)

$$\begin{aligned}
 B_1 &= (\alpha + \delta) (5\alpha^3 + 3\alpha^2\delta - 9\alpha\delta^2 + 32\alpha - 7\delta^3 - 16\delta) \\
 &\quad + 48 + \left([4 + (3\alpha - \delta)(\alpha + \delta)] [(\alpha + \delta)^2 + 4]^2 \right. \\
 &\quad \left. \times (36 - (\alpha + \delta)(\alpha(8\delta(\alpha + \delta) - 19) + 17\delta)) \right)^{1/2}, \quad (26) \\
 B_2 &= 2 \left(2(\alpha^2 + 2)\delta^2 + \alpha(3\alpha^2 + 4)\delta - 4(\alpha^2 + 2) \right. \\
 &\quad \left. - \alpha\delta^3 \right) \times ((\alpha + \delta)^2 + 4). \quad (27)
 \end{aligned}$$

With this data, we can obtain the interpolating solutions which smoothly connect the IR hyperscaling violating geometries to the UV AdS₄ geometries. To connect our analytic IR hyperscaling violating solutions to an asymptotically AdS₄ metric, we numerically solve the Einstein equations from $r = r_0$ to $r = \infty$. Here r_0 is some small radius where the solutions are given by eq. (19) and (20). We solve numerically by setting $V_0 = -1$. At $r = r_0$, the condition $|\epsilon d_i r_0^i| \ll 1$ ($i = 1, 2$) needs to be satisfied [57]. We can obtain the appropriate boundary condition in the UV by fine-tuning ϵ .

The results of interpolating functions $\tilde{a}(r)$, $b(r)$, $\phi(r)$, for the parameter choice $\alpha = -1/3$, $\delta = 0.55$, $\epsilon d_1 = 0.01$ are shown in Fig. 1 - 3. For this parameter choice, we obtain $\gamma \approx 1 - 0.06$, $\beta \approx 0.01$, $k \approx -0.1$, $C_a \approx 1$, $Q_e^2 \approx 0.5$, and we have positive ν , $\nu \approx 0.9 > 0$, and real d_2 and d_3 , $d_2 \approx -1.4 d_1$, $d_3 \approx 0.5 d_1$. The results shown in Fig. 1 - 3 are essentially the same as given in the appendix F of [30].

Similarly in the finite temperature case, we can obtain the interpolating solutions. We now add the x -dependent perturbation on this background to study the stripe stability on the background geometry.

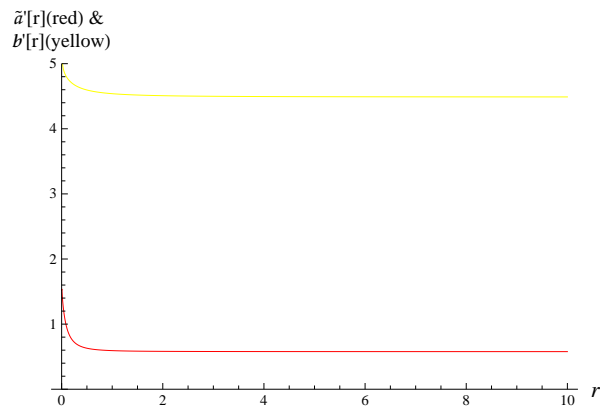


FIG. 2: The interpolating solution $\tilde{a}'(r)$ (red) and $b'(r)$ (yellow) for the same parameter choice. $\lim_{r \rightarrow \infty} \tilde{a}'(r) \rightarrow \frac{1}{\sqrt{3}}$. (color online)

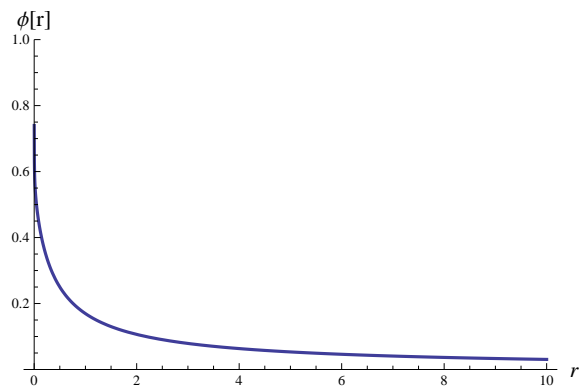


FIG. 3: The interpolating solution $\phi(r)$ for the same parameter choice. $\lim_{r \rightarrow \infty} \phi(r) \rightarrow 0$, for the asymptotic AdS₄ in the UV. (color online)

III. PERTURBATION ANALYSIS IN THE PROBE LIMIT

A. Perturbation equations in the probe limit

Given the full solutions which interpolate between the IR hyperscaling violating geometries and UV AdS₄, we add the x -dependent perturbation and study the onset of the stripe instability. First, for the sake of simplicity, we neglect the graviton fluctuation, namely, we consider the stability in the “probe limit”, where matter fluctuation will not back-react to the graviton fluctuation. In this limit, the translational symmetry breaking can occur and there can exist unstable mode, but the background geometries are fixed. We will see even in this case, we have interesting phenomena for a dynamical instability of the translationally invariant vacuum.

On the background metric and flux given by eq. (8)

and eq. (9), we add the following small fluctuation,

$$\delta A_y \quad , \quad \delta a \quad , \quad \delta \phi, \quad (28)$$

and we choose these fluctuations are x -coordinate dependent. If any of these modes show nonzero vacuum expectation value with the boundary condition that their non-normalizable modes disappear at the boundary, we have gravity dual of the translational symmetry breaking.

From the dilaton fluctuation equation eq. (4), we have

$$\begin{aligned} \frac{4}{\sqrt{-g}} \partial_\mu (\sqrt{-g} g^{\mu\nu} \partial_\nu \delta \phi) &= \partial_\phi^2 V(\phi, a) \delta \phi \\ + (\partial_\phi^2 f(\phi)) F^2 \delta \phi + 2(\partial_\phi f(\phi)) F^{\mu\nu} \delta F_{\mu\nu}. \end{aligned} \quad (29)$$

Note that the third term on the RHS vanish, since $F^{\mu\nu} \neq 0$ only for F^{tr} but we excite only δA_y . Therefore, dilaton equation of motion can be trivially satisfied by setting

$$\delta \phi = 0, \quad (30)$$

so we can set the dilaton fluctuation to be zero. In this paper, we will set the fluctuation of ϕ to be zero, $\delta \phi = 0$. In such case, the operators which are dual to A_y , a can condensate.

The axion fluctuation equation of motion eq. (5) gives

$$\begin{aligned} \frac{4}{\sqrt{-g}} \partial_\mu (e^{2\xi\phi} \sqrt{-g} g^{\mu\nu} \partial_\nu \delta a) \\ = (\partial_a \theta(a)) \epsilon^{\mu\nu\lambda\eta} F_{\mu\nu} \delta F_{\lambda\eta}. \end{aligned} \quad (31)$$

Here we have used the fact that background flux is purely electrical, $F\tilde{F} = 0$.

The gauge field equation of motion eq. (6) yields,

$$\begin{aligned} \partial_\mu \left(\sqrt{-g} (f(\phi) \delta F^{\mu\nu} + \theta(a) \delta \tilde{F}^{\mu\nu} \right. \\ \left. + (\partial_a \theta(a)) \tilde{F}^{\mu\nu} \delta a) \right) = 0, \end{aligned} \quad (32)$$

here we used $\delta \phi = 0$. We need to study the coupled equation for δA_y and δa given by eq. (31) and eq. (32).

We follow the analysis of [41] closely. We set,

$$\delta A_y = \delta A_y(r) \sin qx e^{-i\omega t}, \quad (33)$$

$$\delta a = \delta a(r) \cos qx e^{-i\omega t}. \quad (34)$$

By using the background metric and flux given previously, after a bit algebra, the $\nu = y$ component of eq. (32) gives,

$$\begin{aligned} \sqrt{-g} g^{yy} f(\phi) (-g^{xx} q^2 - g^{tt} \omega^2) \delta A_y(r) \\ + \partial_r (\sqrt{-g} g^{yy} f(\phi) g^{rr} \partial_r \delta A_y(r)) \\ - q \sqrt{-g} (\partial_a \theta(a)) \tilde{F}^{xy} \delta a(r) = 0. \end{aligned} \quad (35)$$

With the metric ansatz eq. (8), and by using $\delta \tilde{F}^{\mu\nu} = 0$, and

$$\sqrt{-g} \tilde{F}^{xy} = \sqrt{-g} \epsilon^{xytr} F_{tr} = -\frac{Q_e}{b^2 f(\phi)}, \quad (36)$$

this equation is re-written as

$$\begin{aligned} f(\phi) (-b^{-2} q^2 + \tilde{a}^{-2} \omega^2) \delta A_y(r) \\ + \partial_r (f(\phi) \tilde{a}^2 \partial_r \delta A_y(r)) \\ + (\partial_a \theta(a)) \frac{q Q_e}{b^2 f(\phi)} \delta a(r) = 0. \end{aligned} \quad (37)$$

Note that both a term proportional to q^2 , and a term induced by axion term, have explicit common factor b^{-2} .

Using $\epsilon^{rxy} = -\epsilon^{xry} = 1/\sqrt{-g}$ and the fact that the background axion takes the zero VEV, it is straightforward to check that $\nu \neq y$ component of eq. (32) is automatically satisfied.

Similarly, the axion fluctuation equation of motion is written as

$$\begin{aligned} e^{2\xi\phi} b^2 (-b^{-2} q^2 + \tilde{a}^{-2} \omega^2) \delta a(r) \\ + \partial_r ((e^{2\xi\phi} b^2) \tilde{a}^2 \partial_r \delta a(r)) \\ + (\partial_a \theta(a)) \frac{q Q_e}{b^2 f(\phi)} \delta A_y(r) = 0. \end{aligned} \quad (38)$$

We will solve the coupled equations eq. (37) and eq. (38) to study the translational symmetry breaking and stability of the translationally invariant vacuum. However since eq. (37) and (38) are coupled, generically it is quite difficult to solve these for the stability. However since there are analytical expressions for the metrics in the IR, which are the hyperscaling violating geometries given by eq. (10) and (11), we first restrict our attention to the near horizon IR geometries.

B. Negative momentum square mode on the hyperscaling violating geometry: finite temperature analysis

First, let's consider the finite temperature case, where the near horizon metric is given by eq. (10) and (11). In the near horizon region, where $r \rightarrow r_h$, we can approximate the metric as

$$\tilde{a}^2 = (2\beta + 2\gamma - 1) C_a^2 r_h^{2\gamma-1} (r - r_h), \quad (39)$$

$$b^2 \rightarrow r_h^{2\beta}, \quad f(\phi) \rightarrow r_h^{2\alpha k}, \quad (40)$$

With this approximation, the eq. (37) and eq. (38) reduce to

$$\begin{aligned} r_h^{2\alpha k} \left(-r_h^{-2\beta} q^2 + \tilde{a}^{-2} \omega^2 \right) \delta A_y(r) \\ + \partial_r (r_h^{2\alpha k} \tilde{a}^2 \partial_r \delta A_y(r)) + c_1 \frac{q Q_e}{r_h^{2\beta+2\alpha k}} \delta a(r) = 0. \end{aligned} \quad (41)$$

$$\begin{aligned} r_h^{2\xi k+2\beta} \left(-r_h^{-2\beta} q^2 + \tilde{a}^{-2} \omega^2 \right) \delta a(r) \\ + \partial_r (r_h^{2\xi k+2\beta} \tilde{a}^2 \partial_r \delta a(r)) + c_1 \frac{q Q_e}{r_h^{2\beta+2\alpha k}} \delta A_y(r) = 0. \end{aligned} \quad (42)$$

It is more convenient to re-write these as

$$\begin{aligned} & \left(-r_h^{-2\beta} q^2 + \tilde{a}^{-2} \omega^2\right) \delta A_y + \partial_r (\tilde{a}^2 \partial_r \delta A_y) \\ & + c_1 \frac{q Q_e}{r_h^{2\beta+4\alpha k}} \delta a = 0, \end{aligned} \quad (43)$$

$$\begin{aligned} & \left(-r_h^{-2\beta} q^2 + \tilde{a}^{-2} \omega^2\right) \delta a + \partial_r (\tilde{a}^2 \partial_r \delta a) \\ & + c_1 \frac{q Q_e}{r_h^{4\beta+2\xi k+2\alpha k}} \delta A_y = 0. \end{aligned} \quad (44)$$

By multiplying $c_2 = r_h^{\beta+\xi k-\alpha k}$ to eq. (44), we obtain

$$\begin{aligned} & \left(-r_h^{-2\beta} q^2 + \tilde{a}^{-2} \omega^2\right) \psi_1 + \partial_r (\tilde{a}^2 \partial_r \psi_1) \\ & + c_1 \frac{q Q_e}{c_2 r_h^{2\beta+4\alpha k}} \psi_2 = 0, \end{aligned} \quad (45)$$

$$\begin{aligned} & \left(-r_h^{-2\beta} q^2 + \tilde{a}^{-2} \omega^2\right) \psi_2 + \partial_r (\tilde{a}^2 \partial_r \psi_2) \\ & + c_1 \frac{q Q_e}{c_2 r_h^{2\beta+4\alpha k}} \psi_1 = 0. \end{aligned} \quad (46)$$

where

$$\delta A_y \equiv \psi_1 \quad , \quad c_2 \delta a \equiv \psi_2 \quad (47)$$

By choosing $\psi_{\pm} \equiv \psi_1 \pm \psi_2$, we have two independent equations

$$\begin{aligned} & \left(-r_h^{-2\beta} q^2 + \tilde{a}^{-2} \omega^2\right) \psi_{\pm} + \partial_r (\tilde{a}^2 \partial_r \psi_{\pm}) \\ & \pm c_1 \frac{q Q_e}{r_h^{3\beta+3\alpha k+\xi k}} \psi_{\pm} = 0. \end{aligned} \quad (48)$$

These equations have very similar structure to the equations of motion for massive scalars in the finite temperature black brane. However due to the axion term proportional to c_1 , it has an ‘‘effective momentum square’’ defined as

$$q_{eff\pm}^2 \equiv q^2 \mp c_1 \frac{q Q_e}{r_h^{\beta+3\alpha k+\xi k}}. \quad (49)$$

We take $c_1 q Q_e > 0$ without loss of generality. Note that this guarantees that at the horizon, one of the ‘‘effective momentum square’’, q_{eff+}^2 above for the mode $\psi_+(r)$, becomes always negative. The minimum value is given at critical wave number q_c ,

$$q_c = \frac{c_1 Q_e}{2 r_h^{\beta+3\alpha k+\xi k}}, \quad (50)$$

with minimum momentum square

$$q_{eff+}^2|_{q=q_c} = -\frac{c_1^2 Q_e^2}{4 r_h^{2(\beta+3\alpha k+\xi k)}} < 0, \quad (51)$$

which is always negative.

This is very similar to the situations where the striped phase instability is studied by [40, 41]; The axion term

$c_1 \neq 0$ makes the system have lower energy by having the nonzero momentum ‘‘stripe’’ type of the spatially modulated mode.

However contrary to the IR AdS₂ case, there are difference on the study of the instability of the IR hyperscaling violating geometries with finite but small temperature; Due to the additional warping factor in hyperscaling violating geometries, there is extra temperature (r_h) dependence for this effective momentum square, and $c_1 Q_e$ appears only in the combinations of $c_1 Q_e / r_h^{\beta+3\alpha k+\xi k}$ [58]. In the AdS₂ case, where $\alpha = \delta = 0$ for $\beta = k = 0$ and $\gamma = 1$ in eq. (12) and (13), $c_1 Q_e$ does not involve any temperature dependence, since $r_h^{\beta+3\alpha k+\xi k}$ becomes constant.

If $c_1 Q_e / r_h^{\beta+3\alpha k+\xi k}$ are very large, for $q \neq 0$, ψ_+ mode can have lower energy with nonzero momentum q mode, and the existence of such negative momentum square mode gives the possibility that such mode induces the instability of the translationally invariant vacuum.

The fact that $c_1 Q_e$ appears in the combinations of $c_1 Q_e / r_h^{\beta+3\alpha k+\xi k}$ implies that the situation is very different, depending on $\beta + 3\alpha k + \xi k$ is positive or negative. If

$$\beta + 3\alpha k + \xi k > 0, \quad (52)$$

as we lower the temperature (*i.e.*, as we lower r_h), the instability are more likely to occur even for the small values of $c_1 Q_e$, due to the enhancement by the factor $1/r_h^{\beta+3\alpha k+\xi k}$. In this case, $c_1 Q_e / r_h^{\beta+3\alpha k+\xi k}$ diverges positively at $r_h \rightarrow 0$ and q_{eff+}^2 goes to negative infinity, and these suggest that the instabilities are expected to occur. On the other hand, if $\beta + 3\alpha k + \xi k$ is negative, as we lower the temperature, we need to increase $c_1 Q_e$ in order to keep the same value for q_{eff+}^2 , due to the suppression by the factor $1/r_h^{\beta+3\alpha k+\xi k}$.

However, whether the existence of the negative effective momentum square mode, $q_{eff+}^2 < 0$, which is evaluated at the horizon, is enough or not for instability is another question. This is because in general hyperscaling violating geometries, we do not know the critical values of the instability. This is in sharp contrast to the AdS₂ case. In the AdS₂ case, partially due to the scale invariance of the geometry, we have a sharp bound for the instability, *i.e.*, Breitenlohner - Freedman (BF) bound. However for geometries with hyperscaling violation, we generically do not expect sharp bound for generic radius and therefore in order to show that there is an unstable mode, local argument is not enough in general and we need to study the full bulk system to search for the unstable mode. Note that since hyperscaling violating geometries are IR limit and they approach AdS₄ in the UV, this means that we need to study the perturbation equations on the whole geometries, with the normalizable boundary condition in the UV AdS₄ region.

However, before we study the full bulk system for the unstable mode numerically, one might wonder if something special occurs for the special parameter range

where the equality of eq. (52) holds. To understand this marginal parameter range in more detail, we continue the study of perturbation equations on the IR hyperscaling violating geometries by taking the zero temperature limit.

C. Zero temperature analysis and instability criteria

1. Zero temperature perturbation

We analyze the instabilities at zero temperature limit, where the metric is

$$\tilde{a}^2 = C_a^2 r^{2\gamma} \quad , \quad b^2 = r^{2\beta} . \quad (53)$$

In this case, by redefining the field as

$$\delta A_y \equiv r^{1-\gamma-\alpha k} \delta \hat{A}_y \quad , \quad \delta a \equiv r^{1-\beta-\gamma-k\xi} \delta \hat{a} , \quad (54)$$

the gauge field and axion equations of motion are written as

$$\nabla^2 \delta \hat{X} = M^2 \delta \hat{X} \quad (55)$$

where

$$\nabla^2 \equiv C_a^2 \partial_r r^2 \partial_r , \quad (56)$$

$$\delta \hat{X} = \begin{pmatrix} \delta \hat{A}_y \\ \delta \hat{a} \end{pmatrix} , \quad M^2 = \begin{pmatrix} A(r) & B(r) \\ B(r) & C(r) \end{pmatrix} , \quad (57)$$

$$A(r) = C_a^2 (-1 + \gamma + \alpha k) (\gamma + \alpha k) + q^2 r^{2-2\beta-2\gamma} , \quad (58)$$

$$B(r) = -c_1 q Q_e r^{2-3\beta-2\gamma-k(3\alpha+\xi)} , \quad (59)$$

$$C(r) = C_a^2 (-1 + \beta + \gamma + k\xi) (\beta + \gamma + k\xi) + q^2 r^{2-2\beta-2\gamma} , \quad (60)$$

where we have set $\omega = 0$, since it allows us to see the instability onset.

Note that if both

$$2 - 3\beta - 2\gamma - k(3\alpha + \xi) < 0 , \quad (61)$$

and

$$2 - 3\beta - 2\gamma - k(3\alpha + \xi) < 2 - 2\beta - 2\gamma , \quad (62)$$

are satisfied, the off-diagonal terms, which are proportional to c_1 and which come from the axion term, dominate at the extremal horizon, $r \rightarrow 0$. In such case, we are forced to have the situation where the matrix M^2 has at least one negative eigenvalue, which goes to negative infinity at $r \rightarrow 0$. Therefore in this parameter range, it is expected that there is an unstable mode for the stripe instability.

On the other hand, if the parameters of hyperscaling violation do not satisfy above inequality (61) and (62), then the matrix M^2 does not always have negative eigenvalue at $r \rightarrow 0$. However even in this case, if we take

large c_1 , then at finite r , M^2 has one eigenvalue which becomes negative at some intermediate radius r . From these, we expect that if inequality (61) and (62) hold, the instability is more likely to occur compared to the case where inequality (61) and (62) do not hold. We will see this actually later in the numerical analysis.

Note that the second condition eq. (62) is equivalent to

$$\beta + 3\alpha k + \xi k > 0 , \quad (63)$$

which is the same as eq. (52), *i.e.*, the second term of effective negative momentum square in eq. (49), dominates at the extremal limit $r_h \rightarrow 0$. The first condition eq. (61) is to guarantee that the off-diagonal term will not vanish at the horizon.

2. Analytical criteria for instability onset for special type of hyperscaling violation

There is a special parameter range in hyperscaling violating geometries, which occurs when the equality of both eq. (61) and (62) are satisfied. This is when ξ , the parameter for the axion kinetic term in eq. (1), is tuned as

$$\xi = -3\alpha - \frac{3\beta + 2\gamma - 2}{k} , \quad (64)$$

and β and γ in the IR hyperscaling violating geometries satisfy the relation

$$\beta + \gamma = 1 . \quad (65)$$

For this special type of hyperscaling violating geometries, we can identify the critical mass just as Breitenlohner - Freedman (BF) bound, since the matrix M^2 , given in eq. (57), becomes independent on the radius r , and therefore constant matrix. From the solution eq. (12) and (13), we can see that if we do not have parameter ξ , the only way to satisfy eq. (64) and (65) are AdS₂ case, *i.e.*, $\beta = 0$ and $\gamma = 1$ case. However for the theories with tuned axion kinetic terms ξ as eq. (64), M^2 becomes constant matrix for one real parameter family of hyperscaling violating geometries with eq. (65), and AdS₂ is a special parameter point in this parameter range.

For such IR geometries with hyperscaling violation satisfying (65), M^2 has two eigenvalues, m_{\pm}^2 ,

$$m_{\pm}^2(q) = \frac{1}{2} \left(A_0 + C_0 \pm \sqrt{(A_0 - C_0)^2 + 4B_0^2} \right) , \quad (66)$$

where

$$A_0 = C_a^2 (-1 + \gamma + \alpha k) (\gamma + \alpha k) + q^2 , \quad (67)$$

$$B_0 = -c_1 q Q_e , \quad (68)$$

$$C_0 = C_a^2 (-1 + \beta + \gamma + k\xi) (\beta + \gamma + k\xi) + q^2 . \quad (69)$$

$\delta \hat{X}$ admits the power law ansatz

$$\delta \hat{X} \sim r^{\Delta} , \quad (70)$$

where Δ satisfies

$$C_a^2 \Delta(\Delta + 1) = m_{\pm}^2(q), \quad (71)$$

and critical values for the instability onset are given when Δ becomes complex [59]. By minimizing $m_{\pm}^2(q)$ with respect to q at $q = q_{min}$, it becomes

$$C_a^2 \Delta(\Delta + 1) = m_{\pm}^2(q_{min}), \quad (72)$$

where q_{min} satisfies $\partial_q m_{\pm}^2(q)|_{q=q_{min}} = 0$. Δ becomes complex when

$$m_{\pm}^2(q_{min}) \leq -\frac{1}{4}C_a^2 \quad (73)$$

holds. In the large $c_1 Q_e$ and q case,

$$m_{\pm}^2(q) \approx q^2 - |c_1 Q_e|q, \quad (74)$$

which allows $q_{min} \approx |c_1 Q_e|/2$, and $m_{\pm}^2(q_{min}) \approx -|c_1 Q_e|^2/4$. Therefore in this case, eq. (73) is satisfied and we have stripe instability.

The special relation eq. (65) is the point where both z and θ diverge (z and θ are given by eq. (17)). More precisely, it is the special point of hyperscaling violation where either $z \rightarrow -\infty$ and $\theta \rightarrow +\infty$, or $z \rightarrow +\infty$ and $\theta \rightarrow -\infty$ holds.

It is interesting to see how above results are different from the AdS₂ case. Let's first consider the AdS₂ case, which is the special limit of above and we take $\alpha = \delta = 0$ so that we have $\beta = 0$, $\gamma = 1$, $k = 0$ in eq. (12), and eq. (13). In such case, A_0 , B_0 , C_0 in eq. (67) - (69) simplifies and we obtain

$$m_{\pm AdS_2}^2(q) = q^2 \pm c_1 q Q_e. \quad (75)$$

This $m_{\pm AdS_2}^2$ is the same effective momentum square $q_{eff\mp}^2$ given in eq. (49). Therefore in AdS₂ case, the onset value of the instability, which we call $c_{min AdS_2}$, is given by the equality of eq. (73) as

$$c_{min AdS_2} = \frac{C_a|_{\alpha=\delta=0}}{Q_e|_{\alpha=\delta=0}} = \sqrt{2}. \quad (76)$$

Here we have used eq. (13) and (14). The stripe instability occurs at $c_1 \geq c_{min AdS_2}$.

Next, we consider non-AdS₂ case. Note that eq. (65) is satisfied when $\alpha = \pm\delta$ from eq. (12) and (13). However since $\alpha = -\delta$ gives $\beta = 0$, $\gamma = 1$, which is AdS₂, we consider $\alpha = \delta$ case. From eq. (12) - (14), in this case the hyperscaling violating geometries are parametrized by only one real parameter α , with

$$\beta = \frac{\alpha^2}{1 + \alpha^2}, \quad \gamma = \frac{1}{1 + \alpha^2}, \quad k = -\frac{\alpha}{1 + \alpha^2}, \quad (77)$$

$$Q_e^2 = -V_0 \frac{1 - \alpha^2}{2(1 + \alpha^2)}, \quad C_a^2 = -V_0, \quad (78)$$

with $V_0 < 0$, and eq. (64) gives

$$\xi = -2\alpha. \quad (79)$$

Then, the eigenvalue $m_{\pm}^2(q)$ of M^2 given by eq. (66) becomes

$$m_{\pm}^2(q) = \frac{1}{2(\alpha^2 + 1)^4} \left(2(\alpha^2 + 1)^4 q^2 - 8(\alpha^2 + 1)^2 \alpha^4 V_0 - \sqrt{2} \sqrt{(\alpha^2 + 1)^6 V_0 ((\alpha^4 - 1) c_1^2 q^2 + 8\alpha^4 V_0)} \right). \quad (80)$$

Since this has minima at

$$q = q_{min} = \frac{\sqrt{-V_0} \sqrt{(1 - \alpha^2)^2 c_1^2 - \frac{64\alpha^4}{c_1^2}}}{2\sqrt{2}(1 - \alpha^4)}, \quad (81)$$

the instability condition eq. (73) becomes

$$\begin{aligned} & \frac{-2\sqrt{(\alpha^2 - 1)^2 (\alpha^2 + 1)^6 c_1^4 V_0}}{8(\alpha^2 + 1)^4} \\ & + \frac{(\alpha^2 + 1)^2 V_0}{8c_1^2 (\alpha^2 - 1)(\alpha^2 + 1)^4} \times \left((\alpha^2 - 1)^2 (\alpha^2 + 1) c_1^4 \right. \\ & \left. - 64(\alpha^6 + \alpha^4) - 32(\alpha^2 - 1)\alpha^4 c_1^2 \right) \leq \frac{V_0}{4}. \quad (82) \end{aligned}$$

Therefore, the onset c_1 value of the instability, which we call c_{min}^{α} , is given by the equality of this and it is

$$c_{min}^{\alpha} = \sqrt{2} \left(\frac{1 + \alpha^2}{1 - \alpha^2} \right)^{1/2}. \quad (83)$$

The instability occurs when $c_1 \geq c_{min}^{\alpha}$, which is larger than the critical value $c_{min AdS_2}$ for AdS₂ case, $\sqrt{2}$. Therefore it is more stable than the AdS₂ case, regarding the stripe instability.

This expression loses its meaning when $\alpha^2 \geq 1$, corresponding to $\gamma \leq 1/2$. But γ cannot be less than $1/2$, since then the entropy density of these black brane are proportional to the negative power of the temperature, which, thermodynamically, does not make sense [60]. Another reason for $\gamma > 1/2$ is that if $\gamma \leq 1/2$, then the null rays from the zero temperature horizon $r = 0$ can reach nonzero r at finite time, which contradicts with the ‘‘horizon’’ property at $r = 0$ [61].

3. $\xi = 0$ case

In the next section, we conduct numerical analysis of generic parameter points where such an equality eq. (65) does not hold. For that purpose, let's investigate the $\xi = 0$ case a bit more, since this is the case where axion has canonical kinetic term.

The parameter range which satisfies eq. (62) is given by

$$(\alpha + \delta)(5\alpha - \delta) < 0, \quad (84)$$

and for eq. (61), it is given by

$$(\alpha + \delta)(3\alpha + \delta) < 0. \quad (85)$$

This gives

$$-3\alpha < \delta < -\alpha \quad (\text{for } \alpha > 0), \quad (86)$$

$$-3\alpha > \delta > -\alpha \quad (\text{for } \alpha < 0). \quad (87)$$

This range is written in terms of β and γ , or θ and z . From eq. (12), we have

$$\alpha = \pm \frac{1 - 2\beta - \gamma}{\sqrt{\beta(1 - \beta)}}, \quad \delta = \pm \frac{\gamma - 1}{\sqrt{\beta(1 - \beta)}}. \quad (88)$$

Remember that we need

$$\frac{1}{2} < \gamma, \quad 0 < \beta < 1. \quad (89)$$

Therefore, the parameter range, eq. (86) or (87), is equivalent to

$$0 < \beta < \frac{1}{3}(1 - \gamma), \quad \frac{1}{2} < \gamma < 1. \quad (90)$$

In terms of θ and z , using

$$\beta = \frac{\theta - 4}{2(\theta - 2z)}, \quad \gamma = \frac{\theta - 4z}{2(\theta - 2z)}, \quad (91)$$

from eq. (17), the parameter range eq. (90) is written as

$$4 < \theta < 6, \quad z < 0. \quad (92)$$

So far we consider the parameter range satisfying eq. (61) and (62). In addition to these, we have more restriction on the parameters. First, we need $\delta k < 0$ which restricts $\delta(\alpha + \delta) > 0$. Second, we want to study the stripe instability on the background which is stable at $q = 0$. Since the IR hyperscaling violating geometries asymptotically approach AdS₄ in the UV, the mass of the dilaton must be above the AdS₄ BF bound for the stability at zero momentum $q = 0$. From our Lagrangian eq. (1), we can read off the mass of the dilaton at $\phi = 0$ and this gives additional constraint

$$-\sqrt{\frac{3}{8}} < \delta < \sqrt{\frac{3}{8}}. \quad (93)$$

Combined these additional conditions with eq. (86) and (87), finally they are summarized as

$$0 > -\frac{1}{3}\delta > \alpha > -\delta > -\sqrt{\frac{3}{8}}. \quad (94)$$

or,

$$0 < -\frac{1}{3}\delta < \alpha < -\delta < \sqrt{\frac{3}{8}}. \quad (95)$$

It is clear that there are parameter ranges satisfying above in the ‘‘physical parameter ranges’’ [62] parametrized by α and δ , as is shown in Figure 1 of [30]. In this parameter range, the effective momentum square

in eq. (51) becomes large negative value at low temperature, and also the off-diagonal components of matrix M^2 in eq. (57) dominates. Therefore it is expected that the instability is more likely to occur at small value of c_1 in this case.

We next conduct numerical analysis for the parameter choice where eq. (94) is satisfied and also for another parameter choice where it is not satisfied. We call the case where eq. (94) is satisfied as case I, and the case where eq. (94) (or eq. (63) in more generic case where $\xi \neq 0$) is not satisfied as case II.

The limit $\alpha \rightarrow 0$ and $\delta \rightarrow 0$ corresponds to the AdS₂ and its stripe instability is well studied in [41, 42]. We will now study numerically the whole bulk system in these parameter range for the stripe instability next.

D. Numerical analysis for the bulk zero mode on the full geometries

Now we conduct numerical investigation of the coupled equations eq. (37) and eq. (38) to study the dynamical translational symmetry breaking. So far we have been concentrating on the perturbation equation analysis restricting our attention on the IR hyperscaling violating geometries. However, now we will conduct the numerical analysis on the full geometries, which approach geometries with hyperscaling violation in the IR and AdS₄ in the UV.

In order to find the onset of the instability, we will look for the zero mode, namely the solution of eq. (37) and eq. (38) with $\omega = 0$. If there is such a zero frequency mode for some value of c_1 , then it is the critical mode. By increasing c_1 above the critical value, the instability occurs. This is because if there is an unstable mode, $\text{Im}(\omega) > 0$ which grows as time evolves, then there should also be zero mode solution $\omega = 0$ at the instability onset point.

Let us emphasize again why searching the zero mode on the full background geometries is important: In the case of IR AdS₂, we have a sharp local criteria for the onset of the stripe instabilities, which is given by the condition $c_1 \geq c_{min AdS_2}$ with eq. (76). This is in contrast to our generic hyperscaling violating geometries in the IR; in two-parameter (β and γ , or θ and z) hyperscaling violating IR geometries, we do not have sharp criteria for the stripe instability from the IR geometries.

However even in the IR AdS₂ case, it is important to find the zero mode on the full geometries which approach AdS₄ in the UV. This is because generically the stability is not determined by the IR region only, but rather it is determined by the full geometries. It is especially so if two modes are coupled.

To see this, let us consider the IR AdS₂ geometries which approach AdS₄ in the UV. For the IR AdS₂ region, the matrix M^2 in eq. (55) becomes constant matrix and we can obtain two eigenvector modes (let us call these as mode A and B) made by some specific linear combination

of mode δA_y and δa . Suppose that the mode A gives the lower eigenvalue of the matrix M^2 than the mode B , and furthermore that the eigenvalue of the mode A is lower than the AdS₂ BF bound and the eigenvalue of the mode B is higher than the AdS₂ BF bound. It is true that if we excite only the mode A , then we can lower the energy by the mode A perturbation and this indicates instability. However due to the UV boundary condition and the mixing of the two modes, generically we cannot excite only the mode A , but rather we need to excite the mode B too in general [63]. At what ratio, we excite the mode A and B , is determined by the full (whole) geometries. Therefore, depending on the ratio of the mode A and B excitations, we can see if the system is unstable or not by the perturbation. This is because the mode A lowers the energy but the mode B increases the energy in the IR AdS₂. In this way, it is generically determined not by the local IR geometry only, but rather by the full geometries. Therefore it is important to find the zero mode on the whole geometries including IR and UV.

Furthermore, in the case of IR hyperscaling violating geometries, which is parametrized by two parameters, we do not generically have sharp BF-like bound. Therefore it is more important to search for the zero mode on the full geometries which include both IR and UV region.

We now seek for the zero mode on the full geometries. For numerics, we set $V_0 = -1$. Introducing new variables $\psi_{\pm} = \delta A_y \pm c_2 \psi_2$ as eq. (47), we can obtain the boundary condition at the horizon $r = r_h$ by imposing regularity as

$$\partial_r \psi_{\pm}|_{r=r_h} = \frac{r_h^{1-2\beta-2\gamma} q_{eff\pm}^2 \psi_{\pm}|_{r=r_h}}{(2\beta + 2\gamma - 1)C_a^2}, \quad (96)$$

where $q_{eff\pm}^2$ is the effective momentum square defined in eq. (49).

In order to find the onset of the spontaneous translational symmetry breaking in the holographic dual setting, we impose Dirichlet boundary condition for the variables δA_y and δa , at the AdS₄ boundary,

$$\delta A_y = \delta a = 0 \quad \text{for} \quad r = \infty. \quad (97)$$

This corresponds to the requirement that there is no non-normalizable mode for δA_y and δa in the UV AdS₄ boundary. Non-normalizable mode for δA_y and δa approach constant in the UV AdS₄.

It is useful to consider the parameter counting. For given fixed parameters α , δ , ξ , r_h , and c_1 , there are two free parameters $\psi_-|_{r=r_h}$ and q . Note that $\psi_+|_{r=r_h}$ is not a free parameter, since we can fix $\psi_+|_{r=r_h}$ to unity without loss of generality in linearized perturbations. We tune $\psi_-|_{r=r_h}$ and q such that the two boundary conditions eq. (97) are satisfied. After this tuning, we have no parameter left, and as a results, we have nonzero normalizable mode for both ψ_+ and ψ_- at $r \rightarrow \infty$. This implies that there are spatially modulated VEV for the

scalar and vector current $\langle j_y \rangle$, which are dual to axion and gauge boson A_y , and this implies that dual theories at IR show the ‘‘current density wave’’ phase. Note also that for a given temperature $T(r_h)$, we expect normalizable zero modes to appear at specific values of momentum q .

As we have discussed, we expect that the effect of the axion term and the negative ‘‘effective momentum square’’ is enhanced or suppressed depending on eq. (94) is satisfied or not. In order to see the difference, we investigate two typical cases; Case I corresponding to $\alpha = -0.33$, $\delta = 0.55$, $\xi = 0$, which gives $\beta = 0.01$, $\gamma = 0.94$, $k = -0.10$, and it satisfies $\beta + 3\alpha k + \xi k > 0$. Case II corresponding to $\alpha = 0.2$, $\delta = 0.55$, $\xi = 0.4$, which gives $\beta = 0.12$, $\gamma = 0.82$, $k = -0.33$, and it satisfies $\beta + 3\alpha k + \xi k < 0$.

It is easily checked that for the case I, it satisfies eq. (94), and therefore, (61) - (63). So case I corresponds to the case where axion term is expected to be enhanced at low temperature $r_h \rightarrow 0$ due to $c_1 Q_e / r_h^{\beta+3\alpha k+\xi k} \rightarrow \infty$, and we expect that axion term induces instability even at very small values of c_1 at low temperature.

On the other hand, for the case II, it violates eq. (94) (more precisely it violates eq. (63) since $\xi \neq 0$), but does not violate the UV AdS₄ BF bound (93). Therefore case II corresponds to the case where axion term is expected to be rather suppressed at low temperature $r_h \rightarrow 0$ due to $c_1 Q_e / r_h^{\beta+3\alpha k+\xi k} \rightarrow 0$, and we expect that we need large values of c_1 in order to induce instability at low temperature.

For both cases, we first numerically construct the background solutions interpolating the IR analytical hyperscaling violating geometries and UV AdS₄ as we reviewed in §IIB2. Then we solve the coupled eq. (37) and eq. (38) and find numerically the solutions ψ_{\pm} satisfying the boundary conditions eq. (97) for a suitable c_1 , q and ψ_- for each temperature $T(r_h)$, where eq. (15) gives the relationship between r_h and T .

For each temperature we find the zero mode solution by tuning q for c_1 , as far as $c_1 > c_{min}$. There is a minimum value c_{min} for c_1 , namely, we could not find any zero mode solution for any q and ψ_- when $c_1 < c_{min}$.

We plot c_{min} for each temperature T in Fig. 4 (case I) and Fig. 5 (case II). As expected, for the case I, c_{min} decreases significantly as T decreases and seems to approach zero. On the other hand, for the case II, c_{min} does not change drastically as T decreases. This suggests that spontaneous translational symmetry breaking easily occurs for much lower temperature when eq. (94) is satisfied, although we cannot further evaluate the minimum value c_{min} for much lower temperature. This is because highly numerical accuracy is required. Similarly we face another difficulties at $\log_{10} T > -3.6$. This is because in such temperature, r_h is not so small and as a result, $\phi|_{r=r_h}$ is not large enough. Then, our perturbative method in §IIB2 to construct full interpolating solutions breaks down. Therefore we conduct numerical analysis in rather restricted low temperature range,

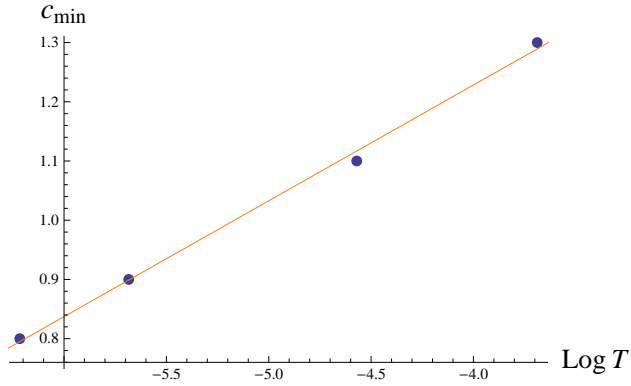


FIG. 4: The plot of c_{min} for various temperatures T for case I ($\alpha = -0.33$, $\delta = 0.55$, $\xi = 0$). Each plot corresponds to $(c_{min}, T, q) = (1.3, 2.05 \times 10^{-4}, 0.83)$, $(1.1, 2.69 \times 10^{-5}, 0.85)$, $(0.9, 2.07 \times 10^{-6}, 0.86)$, $(0.8, 6.08 \times 10^{-7}, 1.0)$. The parameters are approximately on the line $c_{min}(T) = 2.0 + 0.20 \log_{10} T$ in the temperature range we study.

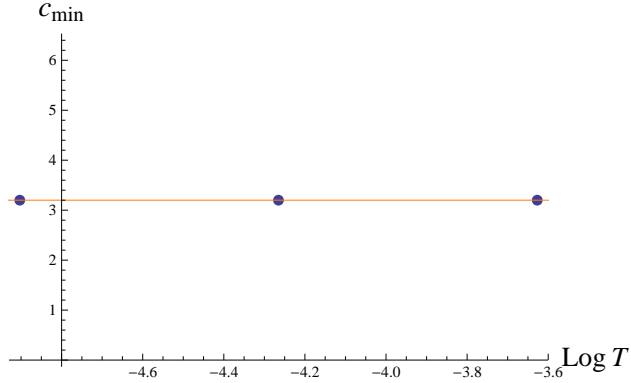


FIG. 5: The plot of c_{min} for various temperatures T for case II ($\alpha = 0.2$, $\delta = 0.55$, $\xi = 0.4$). Each plot corresponds to $(c_{min}, T, q) = (3.2, 2.36 \times 10^{-4}, 0.45)$, $(3.2, 5.43 \times 10^{-5}, 0.45)$, $(3.2, 1.25 \times 10^{-5}, 0.45)$. $c_{min}(T)$ is almost constant, $c_{min}(T) \approx 3.2$ in the temperature range we study.

$-6.3 \lesssim \log_{10} T \lesssim -3.6$ for case I, and $-4.9 \lesssim \log_{10} T \lesssim -3.6$ for case II.

Note that the value range of c_{min} for case I in Fig. 4 is *lower* than the critical value for the AdS₂ case, $c_{min AdS_2} = \sqrt{2}$, which we obtained in eq. (76). This result is consistent with the analysis in §III B and §III C 1 that these are instabilities triggered by the enhanced axion term effect due to the radius dependent factor, $c_1 Q_e / r_h^{\beta+3\alpha k+\xi k} \rightarrow \infty$ at $r_h \rightarrow 0$. One might expect that in case I, at the zero temperature limit where $r_h \rightarrow 0$, the critical value c_{min} approaches zero. Fig. 4 is consistent with this expectation. However due to the numerical difficulties, we could not confirm this at the very low temperature $T \lesssim 6 \times 10^{-7}$.

On the other hand, in case II, we find that the critical value c_{min} is almost constant as we lower the tempera-

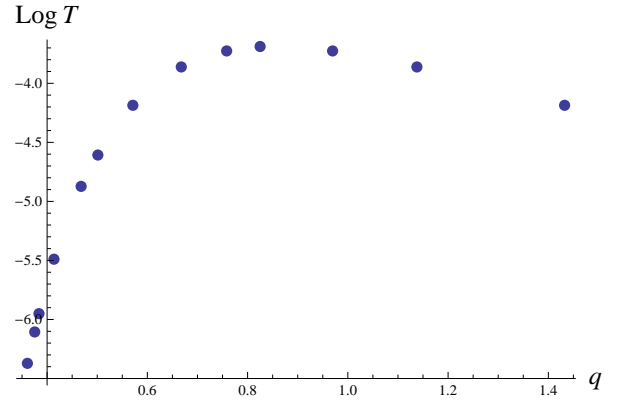


FIG. 6: $T - q$ curve for the normalizable zero mode in full geometries for the case I parameter choice ($\alpha = -0.33$, $\delta = 0.55$, $\xi = 0$), with $c_1 = 1.3$. Due to the “enhancement factor” $1/r_h^{\beta+3\alpha k+\xi k} \approx 8$, even though c_1 is smaller than the critical value for IR AdS₂ case, $c_{min AdS_2} = \sqrt{2}$, we have two q ’s for the zero model, and in between, there should be unstable modes. This figure is in good comparison with IR AdS₂ case analysis done in [41], Figure 2, where, $c_1 > c_{min AdS_2}$.

ture r_h . Note that the value range of c_{min} for case II in Fig. 5 is *higher* than the critical value for the AdS₂ case, suggesting that these are instabilities triggered by the suppressed axion term effect due to the radius dependent factor in case II. However we do not have clear physical interpretation of the result in the case II. From the IR analysis, it might suggest that the critical value c_{min} increases as we lower the temperature, but the result of Fig. 5 is not so. One possible reason for this behavior is that the negative momentum square is more dominating away from the horizon, $r \gg r_h$. As we have discussed in §III C 1, one can see that even in the case II with zero temperature limit, one of the eigenvalue of M^2 can become negative at some finite radius r . In other words, one of the eigenvalue of M^2 can become negative at some finite radius r , but as $r \rightarrow 0$, that value approaches zero. Because of this, even though one of the eigenvalue of M^2 becomes zero at the horizon in the case II, it can become some negative value at some finite radius r and therefore, there could exist a zero mode in the whole bulk for the stripe instability. In such case, if the bulk region, where M^2 eigenvalue becomes negative, is away from the horizon r_h , then it is possible that lowering the temperature does not influence these bulk region much. As a result, in such a case, changing the r_h does not change the c_{min} . However in order to obtain clear physical understanding of these results, we need more detail analysis.

It is also useful to draw the figure for the zero mode in (q, T) plot with fixed c_1 value. [64]. We plot the critical temperatures T versus q for the normalizable zero mode in Fig. 6 (case I parameter choice with $c_1 = 1.3$) and Fig. 7 (case II parameter choice with $c_1 = 3.3$).

In the case I, for given temperature, we generically have two q ’s allowing the normalizable zero modes. Un-

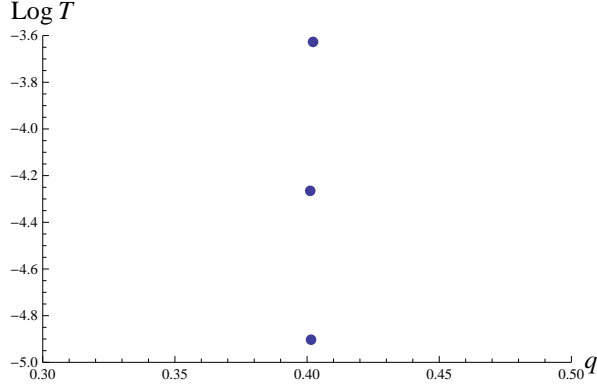


FIG. 7: $T - q$ curve for the normalizable zero mode for the case II parameter choice ($\alpha = 0.2$, $\delta = 0.55$, $\xi = 4$), with $c_1 = 3.3$.

stable modes should exist for momentum q between $q_{\min}(T)$ and $q_{\max}(T)$, and at $T \approx 2.05 * 10^{-4}$, q_{\min} and q_{\max} coincides at $q \approx 0.83$. As we lower the temperature, $q_{\min}(T)$ decreases and $q_{\max}(T)$ increases. In the case I, because $c_1 Q_e / r_h^{\beta+3\alpha k+\xi k}$ goes to infinity at $r_h \rightarrow 0$, we expect to have very large effect of the axion term, and therefore we expect that q_{\max} becomes very large, at zero temperature limit. It would be really nice to confirm this numerically, however we could not conduct numerics at this very low temperature, $T \lesssim 4.2 * 10^{-7}$ due to the difficulties of numerical analysis.

Again in the case II, we do not have clear physical interpretation of the results.

IV. PERTURBATION ANALYSIS BEYOND THE PROBE LIMIT

We have analyzed so far the system without the graviton fluctuation, namely in the probe limit. However, it is pretty straightforward to conduct the similar analysis with the graviton fluctuation, and we will see that the analysis with graviton fluctuation shows essentially the same results, compared with the analysis without graviton. We will see here that there is a negative momentum squared mode in the hyperscaling violating geometry even after we take into account the coupling to the graviton.

We consider again the action (1). The fluctuations we consider are the following components, δg_{ty} , δA_y , δa , $\delta \phi$, and we take the following mode dependence,

$$\delta g_{ty} = \delta g_{ty}(r) \sin qx, \quad (98)$$

$$\delta A_y = \delta A_y(r) \sin qx, \quad (99)$$

$$\delta a = \delta a(r) \cos qx, \quad (100)$$

$$\delta \phi = 0. \quad (101)$$

which has additional graviton mode. Here we have set $\omega = 0$, *i.e.*, no time-dependence from the beginning com-

pared with eq. (33) and (34), in order to discuss the onset of the instability.

Quite analogously to the previous analysis in §III A in the probe limit, given the background geometry eq. (8), we have the equations of motion for the gauge field δA_y ,

$$\begin{aligned} & -f(\phi)b^{-2}q^2\delta A_y(r) \\ & +\partial_r\left(f(\phi)\tilde{a}^2\partial_r\delta A_y(r)+f(\phi)(\partial_r A_t)\delta g_{ty}(r)\right) \\ & +(\partial_a\theta(a))\frac{qQ_e}{b^2f(\phi)}\delta a(r)=0, \end{aligned} \quad (102)$$

and for the axion,

$$\begin{aligned} & \partial_r(e^{2\xi\phi}\sqrt{-g}g^{rr}\partial_r\delta a(r))-q^2e^{2\xi\phi}\sqrt{-g}g^{xx}\delta a(r) \\ & +q(\partial_a\theta(a))F_{tr}\delta A_y(r)=0. \end{aligned} \quad (103)$$

This equation is unmodified by $\delta g_{ty} \neq 0$.

In addition, from the (t, r) component of the trace reversed Einstein equations, we have fluctuation equation for the graviton,

$$\begin{aligned} & \tilde{a}^2b^2\left((\partial_r^2\delta g_{ty}(r))-4f(\phi)F_{tr}(\partial_r\delta A_y(r))\right) \\ & +\left(4\tilde{a}b(\partial_r\tilde{a})(\partial_rb)+b^2(2f(\phi)(F_{tr})^2+V(\phi))\right. \\ & \left.-q^2\right)\delta g_{ty}(r)=0, \end{aligned} \quad (104)$$

and all the other components of Einstein equations and equations of motion are automatically satisfied.

Let's investigate the near horizon limit in similar way to the analysis of §III B and §III C 1. From graviton fluctuation eq. (104), by imposing the regularity condition of the solution at the horizon, we can see that we need the boundary condition $\delta g_{ty}(r=r_h)=0$ at the horizon. Then, it is more convenient to set the new variable $\delta h_{ty}=\partial_r\delta g_{ty}$. And quite analogously to the case where we neglect graviton fluctuation in §III C 1, the three equations eq. (102) - (104) are approximated and written in the near horizon as

$$\hat{\nabla}^2\delta\tilde{Y}|_{r=r_h}\approx\tilde{M}^2|_{r=r_h}\delta\tilde{Y}|_{r=r_h} \quad (105)$$

where

$$\hat{\nabla}^2=\partial_r\tilde{a}^2\partial_r, \quad \delta\tilde{Y}=\begin{pmatrix} \delta A_y \\ \delta a \\ \partial_r(\delta g_{ty}) \end{pmatrix}, \quad (106)$$

and

$$\tilde{M}^2\equiv\begin{pmatrix} q^2/b^2 & (M_{12}(r))^2 & F_{tr} \\ (M_{21}(r))^2 & q^2/b^2 & 0 \\ 4f(\phi)F_{tr}q^2/b^2 & (M_{32}(r))^2 & (M_{33}(r))^2 \end{pmatrix}, \quad (107)$$

$$(M_{12}(r))^2=-\left(\partial_a\theta(a)\right)qF_{tr}/f(\phi), \quad (108)$$

$$(M_{21}(r))^2=-\left(\partial_a\theta(a)\right)qF_{tr}/e^{2\xi\phi}b^2, \quad (109)$$

$$(M_{32}(r))^2=-4\left(\partial_a\theta(a)\right)q(F_{tr})^2, \quad (110)$$

$$(M_{33}(r))^2=\frac{q^2}{b^2}+2f(\phi)(F_{tr})^2-\frac{4ab(\partial_r a)(\partial_r b)}{b^2}-V(\phi), \quad (111)$$

and $\tilde{M}^2|_{r=r_h}$ means \tilde{M}^2 evaluated at the horizon $r = r_h$ [65].

The determinant of \tilde{M}^2 gives

$$\begin{aligned} \text{Det}\tilde{M}^2 &= 4(\partial_a\theta(a))^2 q^2 (F_{tr})^4 e^{-2\xi\phi} b^{-2} \\ &\quad - (\partial_a\theta(a))^2 q^2 (F_{tr})^2 f^{-1}(\phi) e^{-2\xi\phi} b^{-2} (M_{33})^2 \\ &\quad - 4f(\phi) (F_{tr})^2 q^4 b^{-4} + q^4 b^{-4} (M_{33})^2 \\ &= \left(q^4 - \frac{(\partial_a\theta(a))^2 q^2 b^2 (F_{tr})^2}{f(\phi) e^{2\xi\phi}} \right) \\ &\quad \times b^{-4} \left((M_{33})^2 - 4f(\phi) (F_{tr})^2 \right). \end{aligned} \quad (112)$$

From eq. (12) and (13), we can obtain the relation

$$-2\alpha k - 4\beta = 2\delta k = 2\gamma - 2 \quad (113)$$

in the near horizon region of geometries $r \rightarrow r_h$ with hyperscaling violation, where $V(\phi) \rightarrow V_0 e^{2\delta\phi}$, then using eq. (2), (9) - (11), we have

$$\begin{aligned} \text{Det}\tilde{M}^2|_{r=r_h} &= r_h^{-6\beta} \left(q^4 - q^2 c_1^2 Q_e^2 r_h^{-2(\beta+k(3\alpha+\xi))} \right) \\ &\quad \times \left(q^2 - \zeta r_h^{2\gamma+2\beta-2} \right), \end{aligned} \quad (114)$$

where

$$\zeta \equiv 2(Q_e)^2 + 2(2\beta + 2\gamma - 1)\beta C_a^2 + V_0. \quad (115)$$

Therefore, if

$$\beta + k(3\alpha + \xi) > 0, \quad (116)$$

is satisfied, then the axion term proportional to $c_1 Q_e$ dominates. This is exactly the same condition, eq. (52) and eq. (63), which we have obtained in §III B and §III C 1 in the probe limit. In above $\text{Det}\tilde{M}^2$, gauge boson fluctuation δA_y and axion fluctuation δa gives the factor proportional to $(q^4 - q^2 c_1^2 Q_e^2 r_h^{-2(\beta+k(3\alpha+\xi))})$. Note that this is $q_{eff+}^2 \times q_{eff-}^2$ defined by eq. (49). And it is essentially $\text{Det}M^2$ given in eq. (57) - (60), with eq. (61) and (62) at $r \rightarrow 0$ limit, up to overall factor $r^{2(2-2\beta-2\gamma)}$. Therefore even with the graviton fluctuation, δA_y and δa give the same mode for the instability.

The addition of graviton fluctuation, simply adds one more eigenvalue to above $\text{Det}\tilde{M}^2$, and that eigenvalue is proportional to $(q^2 - \zeta r_h^{2\gamma+2\beta-2})$. Therefore, even with the graviton fluctuation, the existence criteria of the negative eigenvalue mode of the matrix $\text{Det}\tilde{M}^2$ due to the axion term is precisely the same as the case without graviton fluctuation; We expect that if (116) is satisfied, the effect of axion term are enhanced as we lower the temperature and intrigues more stripe instability, and the behavior of minimum c_1 for stripe instability is expected to show very similar behavior to the Fig. 4. On the other hand, if (116) is not satisfied, we expect that the effect of axion term are suppressed as we lower the temperature

at the horizon and this intrigues less instability, and the behavior of minimum c_1 for stripe instability is expected to show very similar behavior to the Fig. 5. It would be best if we can confirm this by solving the eq. (102) - (104) numerically with the normalizable boundary condition at the UV AdS₄ boundary as we have done in the probe limit in §III D. However in this case, the parameter range we seek for the normalizable boundary conditions becomes 3-dimensional, instead of 2-dimensional for the probe limit case, and this turns out quite hard task. Therefore we leave this as future work on this paper.

Clearly at the large c_1 limit, we can have a mode which has large negative eigenvalue at some radius, and this indicates the striped phase instability can occur. One difference, compared to the probe limit, is that the analysis for the analytic expression for the onset of the instability in §III C 2 does not work. This is because even if both eq. (64) and (65) hold, the determinant of the matrix \tilde{M}^2 is proportional to $r^{-6\beta}$. So we need $\beta = 0$ and $\gamma = 1$ for the matrix \tilde{M}^2 to become constant matrix, which is AdS₂ case. This implies that we need to introduce one more parameter in the Lagrangian to be tuned, so that we can have constant matrix \tilde{M}^2 in the presence of graviton.

V. SUMMARY AND DISCUSSION

In this paper, we studied the stripe instabilities (spatially modulated instabilities) of the geometries with hyperscaling violation in the IR, which approach AdS₄ metric in the UV asymptotically. The instabilities are induced by the axion term $\delta S = \int d^4 x c_1 a F \wedge F$ in the bulk 4d action. We first study the perturbation equations in the probe limit, and saw that there is a strong correlation between the stripe instabilities caused by the axion term and parameters of the theories which determine the hyperscaling violation. Contrary to the IR AdS₂ case, we found that, due to the lack of scale invariance and the nontrivial radial dependence of the IR hyperscaling violating geometries, the effect of axion term can be either enhanced or suppressed depending on the parameters. In the parameter range where the effect of the axion term is expected to be enhanced, the stripe instability occurs and c_{min} decreases as we lower the temperature, where c_{min} is the critical value for the instability and instability occurs only at $c_1 \geq c_{min}$. On the other hand, in the parameter range where the effect of axion term is expected to be suppressed, we find that c_{min} does not change much as we lower the temperature. We have explicitly obtained the zero mode solutions for the coupled fluctuations of gauge boson δA_y and axion δa numerically in the probe limit, with the boundary condition that there are no non-normalizable modes. This implies that in the dual field theories, the scalar and vector current $\langle j_y \rangle$, which are dual to axion a and gauge boson A_y in the bulk, acquire the spatially modulated VEV spontaneously, and that dual theories at IR show the ‘‘current density wave’’ phase. We identify the instability onset on a certain one-

parameter family of the hyperscaling violating geometries analytically, where the relation eq. (65) holds. We also argue that quite analogous results are expected to hold beyond the probe limit.

There are several open issues which should be understood in better way. We have done our search of the zero mode on rather limited temperature range in §III D. This is due to the numerical difficulties, and it comes from the fact that our background solutions, which are hyperscaling violating geometries in IR and approach AdS₄ in UV, are constructed only numerically. If we could construct an analytical solution, we can search numerically for the zero mode more accurately. So it is interesting and important to look for analytical background solutions which interpolate between UV AdS₄ and IR hyperscaling violating geometries. By conducting the numerical analysis in better way, we can check if the c_{min} goes to zero or not in the zero temperature limit in Fig. 4. Similarly, we can check how the $T - q$ curve behaves in the zero temperature limit in Fig. 6. It is interesting to check these.

We argue in §IV that the results of instability analysis are essentially the same by taking into account the graviton effects. Of course, it is better if we could confirm this by searching for the zero mode explicitly on the full geometries, as we have done in §III D in the probe limit.

There are other issues which we would like to understand in better way. In this paper, we did not argue the validity of the action eq. (1) for the background solutions. However, it can happen that the starting action is not valid for describing the solutions, depending on the behavior of the solutions. For example, our background dilaton has run-away behavior, and if the background dilaton runs to the strong coupling direction in IR, then we have to worry about the possibility that our starting action is highly corrected due to the strong coupling effects. Such a possibility exists if the starting action is derived under the weak coupling approximation. For example, from our action eq. (1), the effective coupling of the gauge field $g_{U(1)}$ is given by $g_{U(1)}^{-2} \equiv f(\phi) = e^{2\alpha\phi}$. In our background solution this behaves as $g_{U(1)} \rightarrow r^{-\alpha k}$ in IR. If we assume that our theory eq. (1) is derived under the weak coupling condition, this with eq. (13) forces us $-\alpha k \propto \alpha(\alpha + \delta) > 0$ for consistency. But this implies that our condition eq. (84) and (85), for the case $\xi = 0$, cannot be satisfied. And we have only the parameter range where the axion term is expected to be suppressed, which corresponds to case II in the analysis of §III D. These issues should be understood more from the string theory embedding view point. However rather in this paper, we study the stability analysis with the assumption that the action eq. (1) is valid for any solutions, we do not “derive” our action eq. (1) from string theory. It would be nice to study these consistency points in more detail.

It could be that if the background dilaton blows up in the IR hyperscaling violating geometries, then we need to take into account the higher loop corrections and this

might make the geometries into the AdS₂ metric in further IR, as studied, for examples, in [51–53]. This viewpoint resolves the problematic singularities of the zero temperature limit of the hyperscaling violating geometries at $r \rightarrow 0$ [66]. However, it is not clear if this is always the case. For examples, once higher loop corrections (corresponds to higher string coupling g_s corrections) enter the game, we always need to worry about full loop correction effects. Namely, once we face the situations where higher order g_s effects are as important as leading order in g_s expansion, this implies that g_s expansion is no more valid. But in general, we do not have such a fully non-perturbative effective action, and the validity of the loop corrected effective action in order to derive the deep IR AdS₂ metric is unclear.

Another interesting question is the end point of the stripe instability. In this paper, we studied the onset of the stripe instabilities. However to see what is the end point of these instabilities, perturbation analysis is not enough. We need to study the equations of motion where A_y and a are coupled in the probe limit, and the full back reacted Einstein equations to go beyond the probe limit. For successful examples of the end point of stripe instabilities, see [40, 42, 46].

In the probe limit, we identify the onset of the stripe instability when the relation eq. (65) holds. It is interesting to note that this relation also holds at the transition point between quasi-particle picture holds/breaks down from the study of the fermion Green’s function on these background [30]. It is interesting to investigate to see if there are any deep reason for this coincident.

There are many open questions to be understood better. However one thing which is very clear is that these geometries with hyperscaling violation and stripe instabilities are rich subject and it is worth understanding more in great detail. We hope to return these questions in future.

Note added: When we have almost finished preparing for the draft, a paper appeared [54], where they also studied the stripe instability on the hyperscaling violating geometries. However our set-up and analysis is different from the one in [54]. The authors of [54] studied the geometries whose IR ($r \rightarrow 0$) is AdS₂, and in large r , they approach the hyperscaling violating geometries. They identified the onset of stripe instability in this IR AdS₂ region by using the AdS₂ BF bound, *i.e.*, local AdS₂ argument. Then they interpret that onset in terms of the large r hyperscaling violating parameters. On the other hand, in this paper we studied the geometries whose IR are hyperscaling violating geometries, which interpolate to the AdS₄ in the UV.

Acknowledgments

We would like to thank Sera Cremonini, Aristomenis Donos, Jerome Gauntlett, Koji Hashimoto, and

Annamaria Sinkovics for helpful discussion and comments/questions on the draft. N.I. would like to thank ICTP South American Institute for Fundamental Re-

search for kind hospitality where part of this work was done. K.M. is supported in part by MEXT/JSPS KAKENHI Grant Number 23740200.

-
- [1] J. M. Maldacena, “The Large N limit of superconformal field theories and supergravity,” *Adv. Theor. Math. Phys.* **2**, 231 (1998) [*Int. J. Theor. Phys.* **38**, 1113 (1999)] [hep-th/9711200].
- [2] E. Witten, “Anti-de Sitter space and holography,” *Adv. Theor. Math. Phys.* **2**, 253 (1998) [hep-th/9802150].
- [3] S. S. Gubser, I. R. Klebanov and A. M. Polyakov, “Gauge theory correlators from noncritical string theory,” *Phys. Lett. B* **428**, 105 (1998) [hep-th/9802109].
- [4] H. Liu, J. McGreevy and D. Vegh, “Non-Fermi liquids from holography,” *Phys. Rev. D* **83**, 065029 (2011) [arXiv:0903.2477 [hep-th]].
- [5] T. Faulkner, H. Liu, J. McGreevy and D. Vegh, “Emergent quantum criticality, Fermi surfaces, and AdS(2),” *Phys. Rev. D* **83**, 125002 (2011) [arXiv:0907.2694 [hep-th]].
- [6] M. Cubrovic, J. Zaanen and K. Schalm, “String Theory, Quantum Phase Transitions and the Emergent Fermi-Liquid,” *Science* **325**, 439 (2009) [arXiv:0904.1993 [hep-th]].
- [7] S. S. Gubser, “Breaking an Abelian gauge symmetry near a black hole horizon,” *Phys. Rev. D* **78**, 065034 (2008) [arXiv:0801.2977 [hep-th]].
- [8] S. A. Hartnoll, C. P. Herzog and G. T. Horowitz, “Building a Holographic Superconductor,” *Phys. Rev. Lett.* **101**, 031601 (2008) [arXiv:0803.3295 [hep-th]].
- [9] S. A. Hartnoll, C. P. Herzog and G. T. Horowitz, “Holographic Superconductors,” *JHEP* **0812**, 015 (2008) [arXiv:0810.1563 [hep-th]].
- [10] C. P. Herzog, “Lectures on Holographic Superfluidity and Superconductivity,” *J. Phys. A A* **42**, 343001 (2009) [arXiv:0904.1975 [hep-th]].
- [11] G. T. Horowitz, “Introduction to Holographic Superconductors,” arXiv:1002.1722 [hep-th].
- [12] G. T. Horowitz and M. M. Roberts, “Zero Temperature Limit of Holographic Superconductors,” *JHEP* **0911**, 015 (2009) [arXiv:0908.3677 [hep-th]].
- [13] G. T. Horowitz, J. E. Santos and D. Tong, “Optical Conductivity with Holographic Lattices,” *JHEP* **1207**, 168 (2012) [arXiv:1204.0519 [hep-th]].
- [14] G. T. Horowitz, J. E. Santos and D. Tong, “Further Evidence for Lattice-Induced Scaling,” *JHEP* **1211**, 102 (2012) [arXiv:1209.1098 [hep-th]].
- [15] N. Iizuka and K. Maeda, “Towards the Lattice Effects on the Holographic Superconductor,” *JHEP* **1211**, 117 (2012) [arXiv:1207.2943 [hep-th]].
- [16] S. A. Hartnoll, D. M. Hofman and A. Tavanfar, “Holographically smeared Fermi surface: Quantum oscillations and Luttinger count in electron stars,” *Europhys. Lett.* **95**, 31002 (2011) [arXiv:1011.2502 [hep-th]].
- [17] S. Sachdev, “A model of a Fermi liquid using gauge-gravity duality,” *Phys. Rev. D* **84**, 066009 (2011) [arXiv:1107.5321 [hep-th]].
- [18] L. Huijse, S. Sachdev and B. Swingle, “Hidden Fermi surfaces in compressible states of gauge-gravity duality,” *Phys. Rev. B* **85**, 035121 (2012) [arXiv:1112.0573 [cond-mat.str-el]].
- [19] L. Huijse and S. Sachdev, “Fermi surfaces and gauge-gravity duality,” *Phys. Rev. D* **84**, 026001 (2011) [arXiv:1104.5022 [hep-th]].
- [20] N. Iqbal and H. Liu, “Luttinger’s Theorem, Superfluid Vortices, and Holography,” *Class. Quant. Grav.* **29**, 194004 (2012) [arXiv:1112.3671 [hep-th]].
- [21] K. Hashimoto and N. Iizuka, “A Comment on Holographic Luttinger Theorem,” *JHEP* **1207**, 064 (2012) [arXiv:1203.5388 [hep-th]].
- [22] T. Senthil, S. Sachdev and M. Vojta, *Phys. Rev. Lett.* **90**, 216403 (2003) [arXiv:cond-mat/0209144].
- [23] S. Sachdev, “Holographic metals and the fractionalized Fermi liquid,” *Phys. Rev. Lett.* **105**, 151602 (2010) [arXiv:1006.3794 [hep-th]].
- [24] N. Iizuka, S. Kachru, N. Kundu, P. Narayan, N. Sircar and S. P. Trivedi, “Bianchi Attractors: A Classification of Extremal Black Brane Geometries,” *JHEP* **1207**, 193 (2012) [arXiv:1201.4861 [hep-th]].
- [25] N. Iizuka, S. Kachru, N. Kundu, P. Narayan, N. Sircar, S. P. Trivedi and H. Wang, “Extremal Horizons with Reduced Symmetry: Hyperscaling Violation, Stripes, and a Classification for the Homogeneous Case,” arXiv:1212.1948 [hep-th].
- [26] S. Kachru, X. Liu and M. Mulligan, “Gravity Duals of Lifshitz-like Fixed Points,” *Phys. Rev. D* **78**, 106005 (2008) [arXiv:0808.1725 [hep-th]].
- [27] M. Taylor, “Non-relativistic holography,” arXiv:0812.0530 [hep-th].
- [28] K. Goldstein, S. Kachru, S. Prakash and S. P. Trivedi, “Holography of Charged Dilaton Black Holes,” *JHEP* **1008**, 078 (2010) [arXiv:0911.3586 [hep-th]]; K. Goldstein, N. Iizuka, S. Kachru, S. Prakash, S. P. Trivedi and A. Westphal, “Holography of Dyonically Dilaton Black Branes,” *JHEP* **1010**, 027 (2010) [arXiv:1007.2490 [hep-th]].
- [29] C. Charmousis, B. Gouteraux, B. S. Kim, E. Kiritsis and R. Meyer, “Effective Holographic Theories for low-temperature condensed matter systems,” *JHEP* **1011**, 151 (2010) [arXiv:1005.4690 [hep-th]]; B. Gouteraux and E. Kiritsis, “Generalized Holographic Quantum Criticality at Finite Density,” *JHEP* **1112**, 036 (2011) [arXiv:1107.2116 [hep-th]].
- [30] N. Iizuka, N. Kundu, P. Narayan and S. P. Trivedi, “Holographic Fermi and Non-Fermi Liquids with Transitions in Dilaton Gravity,” *JHEP* **1201**, 094 (2012) [arXiv:1105.1162 [hep-th]].
- [31] N. Ogawa, T. Takayanagi and T. Ugajin, “Holographic Fermi Surfaces and Entanglement Entropy,” *JHEP* **1201**, 125 (2012) [arXiv:1111.1023 [hep-th]].
- [32] L. Huijse, S. Sachdev and B. Swingle, “Hidden Fermi surfaces in compressible states of gauge-gravity duality,” *Phys. Rev. B* **85**, 035121 (2012) [arXiv:1112.0573 [cond-mat.str-el]].
- [33] E. Shaghoulian, “Holographic Entanglement Entropy and Fermi Surfaces,” *JHEP* **1205**, 065 (2012)

- [arXiv:1112.2702 [hep-th]].
- [34] X. Dong, S. Harrison, S. Kachru, G. Torroba and H. Wang, “Aspects of holography for theories with hyperscaling violation,” *JHEP* **1206**, 041 (2012) [arXiv:1201.1905 [hep-th]].
- [35] E. Perlmutter, “Domain Wall Holography for Finite Temperature Scaling Solutions,” *JHEP* **1102**, 013 (2011) [arXiv:1006.2124 [hep-th]]; E. Perlmutter, “Hyperscaling violation from supergravity,” *JHEP* **1206**, 165 (2012) [arXiv:1205.0242 [hep-th]].
- [36] K. Narayan, “On Lifshitz scaling and hyperscaling violation in string theory,” *Phys. Rev. D* **85**, 106006 (2012) [arXiv:1202.5935 [hep-th]].
- [37] M. Edalati, J. F. Pedraza and W. Tangarife Garcia, “Quantum Fluctuations in Holographic Theories with Hyperscaling Violation,” *Phys. Rev. D* **87**, 046001 (2013) [arXiv:1210.6993 [hep-th]].
- [38] P. Bueno, W. Chemissany and C. S. Shahbazi, “On hvLif-like solutions in gauged Supergravity,” arXiv:1212.4826 [hep-th].
- [39] N. Iizuka and K. Maeda, “Study of Anisotropic Black Branes in Asymptotically anti-de Sitter,” *JHEP* **1207**, 129 (2012) [arXiv:1204.3008 [hep-th]].
- [40] S. Nakamura, H. Ooguri and C. -S. Park, “Gravity Dual of Spatially Modulated Phase,” *Phys. Rev. D* **81**, 044018 (2010) [arXiv:0911.0679 [hep-th]]; H. Ooguri and C. -S. Park, “Holographic End-Point of Spatially Modulated Phase Transition,” *Phys. Rev. D* **82**, 126001 (2010) [arXiv:1007.3737 [hep-th]]; H. Ooguri and C. -S. Park, “Spatially Modulated Phase in Holographic Quark-Gluon Plasma,” *Phys. Rev. Lett.* **106**, 061601 (2011) [arXiv:1011.4144 [hep-th]].
- [41] A. Donos and J. P. Gauntlett, “Holographic striped phases,” *JHEP* **1108**, 140 (2011) [arXiv:1106.2004 [hep-th]].
- [42] A. Donos, J. P. Gauntlett and C. Pantelidou, “Spatially modulated instabilities of magnetic black branes,” *JHEP* **1201**, 061 (2012) [arXiv:1109.0471 [hep-th]]; A. Donos and J. P. Gauntlett, “Holographic helical superconductors,” *JHEP* **1112**, 091 (2011) [arXiv:1109.3866 [hep-th]]; A. Donos and J. P. Gauntlett, “Helical superconducting black holes,” *Phys. Rev. Lett.* **108**, 211601 (2012) [arXiv:1203.0533 [hep-th]]; A. Donos and J. P. Gauntlett, “Black holes dual to helical current phases,” arXiv:1204.1734 [hep-th].
- [43] R. Flauger, E. Pajer and S. Papanikolaou, “A Striped Holographic Superconductor,” *Phys. Rev. D* **83**, 064009 (2011) [arXiv:1010.1775 [hep-th]].
- [44] J. A. Hutasoit, G. Siopsis and J. Therrien, “Conductivity of Strongly Coupled Striped Superconductor,” arXiv:1208.2964 [hep-th].
- [45] N. Jokela, M. Jarvinen and M. Lippert, “Fluctuations and instabilities of a holographic metal,” arXiv:1211.1381 [hep-th].
- [46] M. Rozali, D. Smyth, E. Sorkin and J. B. Stang, “Holographic Stripes,” arXiv:1211.5600 [hep-th].
- [47] A. Donos, J. P. Gauntlett, J. Sonner and B. Withers, “Competing orders in M-theory: superfluids, stripes and metamagnetism,” arXiv:1212.0871 [hep-th].
- [48] T. Hertog and G. T. Horowitz, “Towards a big crunch dual,” *JHEP* **0407**, 073 (2004) [hep-th/0406134].
- [49] N. Iizuka, N. Kundu, P. Narayan, N. Sircar and S. P. Trivedi, 2011, unpublished note.
- [50] J. Gath, J. Hartong, R. Monteiro and N. A. Obers, “Holographic Models for Theories with Hyperscaling Violation,” arXiv:1212.3263 [hep-th].
- [51] S. Harrison, S. Kachru and H. Wang, “Resolving Lifshitz Horizons,” arXiv:1202.6635 [hep-th].
- [52] J. Bhattacharya, S. Cremonini and A. Sinkovics, “On the IR completion of geometries with hyperscaling violation,” arXiv:1208.1752 [hep-th].
- [53] N. Kundu, P. Narayan, N. Sircar and S. P. Trivedi, “Entangled Dilaton Dyons,” arXiv:1208.2008 [hep-th].
- [54] S. Cremonini and A. Sinkovics, “Spatially Modulated Instabilities of Geometries with Hyperscaling Violation,” arXiv:1212.4172 [hep-th].
- [55] One can also construct black brane solutions which do not have large entropy by admitting spatial anisotropy, see for example, [39].
- [56] This solution is obtained under the assumption $Q_e \neq 0$. For the case $Q_e = 0$, the derivation of this solution in [30] breaks down since we do not have to require the condition eq. (2.19) in [30]. Actually AdS₄ is such a limit, where we have $\beta = 1$, $\gamma = 1$, $k = 0$, $\delta = 0$, $C_a^2 = -V_0/6$ and $Q_e = 0$ with arbitrary choice of α .
- [57] In the asymptotic AdS₄ region, ϕ behaves as $\phi \simeq D_+ r^{\lambda_+} + D_- r^{\lambda_-}$ at $r \rightarrow \infty$, where $\lambda_{\pm} = -3/2 \pm \sqrt{9 - 24\delta^2}/2$. As shown in [48], the theory is generally unstable for the perturbation with respect to ϕ when both modes exist. However for the perturbation analysis we conduct in this paper, the dilaton ϕ does not fluctuate. Therefore we consider that the instability of [48] is not related to the stripe instability we investigate in this paper. In addition, for the numerical analysis in §III D, we choose D_+ as small as possible in the range $|\epsilon_i r_0^i| \ll 1$ ($i = 1, 2$).
- [58] Q_e is actually not a parameter, since it takes definite value as eq. (13).
- [59] This simple method gives the generalized Breitenlohner - Freedman (BF) bound for the stability in non-AdS case, for examples, [49, 50].
- [60] See eq. (15), if $\gamma < 1/2$, then $r_h \rightarrow 0$ with $T \rightarrow \infty$.
- [61] We thank Noriaki Ogawa for pointing this out to us.
- [62] “Physical” in the sense that $Q_e^2 > 0$, $C_a^2 > 0$, $\gamma > 0$, $\gamma - \beta > 0$, $\beta > 0$, and $\delta k < 0$ are satisfied.
- [63] To see this, note that in the UV, we can similarly construct the matrix M^2 from the equations of motion for δA_y and δa . The eigenvector mode in the UV (let us call these as A' and B') are different from the eigenvector mode A and B (defined in IR) generically since the metric is different in UV and IR. The mode A' and B' are specific linear combinations of the mode A and B . Now we need to impose boundary condition both at the IR horizon and UV boundary. At the horizon, we have ingoing boundary conditions or regularity condition for both A and B , and at the UV boundary we impose that non-normalizable mode vanishes for both A' and B' . Since for the second order differential equations, we have imposed two boundary conditions (one at the horizon and one at the boundary), we do not have parameter left and this generically implies that we are forced to have excitation both mode A and B in the IR near horizon region generically.
- [64] We thank Aristos Donos and Jerome Gauntlett for raising this question to us.
- [65] In order to derive this result, we have used two conditions; 1) terms proportional to δg_{ty} , are neglected

since $\delta g_{ty}|_{r=r_h} \rightarrow 0$, and 2) using the regularity of the flux F_{tr} and dilaton $f(\phi)$ at the finite temperature horizon $r = r_h$, we can neglect term proportional to $\partial_r \delta A_y(r)$ since $|[(\partial_r(f(\phi)F_{tr}))\tilde{a}^2 \partial_r \delta A_y(r)]|_{r=r_h}| \ll |[f(\phi)F_{tr}(\partial_r \tilde{a}^2) \partial_r \delta A_y(r)]|_{r=r_h}|$ holds.

[66] This singularities can be avoided by introducing small but non-zero temperature. And our studies of the stripe instability in small but non-zero temperature case are not affected by this singularities.